Hindawi Publishing Corporation
Mathematical Problems in Engineering
Volume 2013, Article ID 712723, 11 pages
http://dx.doi.org/10.1155/2013/712723

Research Article

Sliding Mode Control for Diesel Engine Air Path Subject to Matched and Unmatched Disturbances Using Extended State Observer

Sofiane Ahmed Ali and Nicolas Langlois

IRSEEM Technopôle du Madrillet, BP 10024, 76801 Saint-Étienne-du-Rouvray, France

Correspondence should be addressed to Sofiane Ahmed Ali; sofiane.ahmedali@esigelec.fr

Received 2 August 2013; Accepted 22 September 2013

Academic Editor: Xudong Zhao

The paper develops a sliding mode controller via nonlinear disturbance observer for diesel engine air path system subject to matched and unmatched disturbances. The proposed controller is based upon a novel nonlinear disturbance observer (NDO) structure which uses the concept of total disturbance estimation in order to estimate simultaneously the matched and the unmatched disturbances in the system. This estimation is then incorporated in a composite controller which alleviates the chattering problem and maintains the nominal performance of the system in the absence of disturbances. Simulations results of the proposed controller on a recently validated experimental air path diesel engine model show that the proposed methods exhibit a better performances comparing to the baseline SMC in terms of reducing chattering and nominal performances recovery.

1. Introduction

Comparing to gasoline engines, diesel engines have the advantage of producing the requested torque under an optimal compromise between fuel consumption and given exhaust legislation emission level. To meet the requirements of emission standards EURO V and VI, the emissions of diesel engines, particularly oxides of nitrogen (NO_x) and particulate matter (PM), must be controlled at every engine cycles. Earlier reduction mechanism suggested that NO_x emissions can be reduced by increasing the intake manifold exhaust gas recirculation (EGR) fraction and smoke can be reduced by increasing the air/ruel ratio (AFR) [1]. The EGR and the AFR rates are controlled by the EGR and the variable geometry turbine (VGT) actuators whose position determines the amount of the EGR flow in the intake manifold and thus controls the AFR and the EGR ratios variables. The VGT and the EGR actuators are strongly coupled so that conventional calibration/mapping based approaches, which use traditional PI controllers, face difficulty to produce satisfactory and robust results in terms of torque responses, engine-out emission at steady, and transient state conditions, even with very time-consuming and detailed calibrations effort.

With the development of microprocessor technology, especially digital signal processors (DSPs), electronic control units (ECUs) gained in terms of computational capacities so that sophisticated control approaches which achieve smooth, fast, and robust transient operations were more and more introduced in controlling modern diesel engines. Considerable research efforts have been dedicated to the control of modern diesel engines. Several controllers were proposed in the literature, for example, Lyapunov control design [2], robust gain-scheduled controller based on a linear parameter-varying (LPV) model for turbocharged diesel engine [3–5], Indirect passivation [6], predictive control [7], and feedback linearization [8, 9].

Most of these algorithms are control-oriented models; that is, the control laws computed by these algorithms are based upon a model of the diesel engine air path. In the past decade, many TDE air path models were developed and presented in [2, 10–13]. In [2], the authors developed a full-seventh-order TDE air path model which describes the dynamics of several variables such as the pressures and the

oxygen mass fractions in the intake and exhaust manifolds, the turbocharger speed, and the two states of the control signals describing the EGR and the VGT actuator dynamics. To simplify the control design, and due to the fact that the oxygen mass fraction variables are difficult to measure, the seventh-order model is reduced to a third-order one. This simplification leads to the appearance of discrepancies between the description model and the real system due to the neglected dynamics, the model parametric uncertainties, and the potential faults which can occur in the diesel engine air path. Modeling uncertainties arise from sources such as uncertainties on engines cartographies, unmodeled dynamics, and external or internal disturbances. Engine faults affect the TDE air path components. For example, a leakage occurring on the EGR actuators is a fault that affects the performance of any designed controller based on the previous cited methods. In this work, both modeling uncertainties and actuator faults are considered as internal and external disturbances acting on the system via different channels. Indeed, the actuator faults naturally satisfy the so-called matching condition since they act on the control inputs. Modeling uncertainties are unmatched disturbances since they act on different channels from the control input and hence do not satisfy this matching condition. The main objective of this paper is to design an efficient controller which is robust facing the matched and the unmatched disturbances which affects the diesel engine air path.

Sliding mode control [14–17] is a very popular strategy for controlling uncertain nonlinear system. Due to its conceptual simplicity and its capability to reject disturbances and model uncertainties, SMC strategies are widely employed in industrial applications including robotic manipulator systems [18–20], electrical machines [21, 22], power converters [23, 24], and flight control systems [25, 26]. Despite these attractive features, the major drawback of the traditional SMC controllers is that they are only insensitive to matched disturbance [27], while unmatched disturbance affects severely the sliding motion, and the well-known robustness of SMC does not hold any more. To overcome this difficulty, many researchers devoted themselves to the control design for uncertain system under mismatched disturbances.

Generally speaking, the matched and the unmatched disturbances in control systems are unmeasurable; thus, a disturbance observer is needed for the disturbance attenuation. Disturbance observers can be classified into the following two categories. The first category is a model based disturbance observer in which the designer needs to know about the model of the plant. Many model based disturbance observers were proposed in the literature including unknown input observer (UIO) [28], the disturbance observer (DOB) [29, 30], the perturbation observer [31], the equivalent input disturbance (EID) based estimation [32], and the sliding mode observer (SMO) which was primarily designed for robust state estimation and then has been extended to estimate unknown inputs or faults by reconstructing the disturbance using the so-called "equivalent output error injection" [33]. The second category is referred to as extended state observers (ESOs) [34–37] which is characterized by a promising features due to the least amount of plant information needed for their implementation. Comparing to model based disturbance observers, (ESOs) techniques need only to know the system order and hence are more robust and easy to implement from a practical point of view. However, standard (ESO) observers suffer from one major drawback coming from the fact that they are only available for integral chain systems, thus not applicable for more general class of system such as flight control system. In addition, the unmatched disturbances are no longer available for these standard ESO techniques. Recently in [38], the authors generalized the concept of ESO to nonintegral chain systems subject to mismatched disturbances.

To alleviate the well-known problem of chattering and retain the nominal control for the SMC in presence of matched and unmatched disturbances, SMC disturbance based feedforward control which combines a disturbance observer (DOB) with an SMC feedback control was developed for matched disturbances in [39–43] and recently in [44] for the unmatched ones. However, in this work, the considered diesel engine air path faces simultaneously the matched and the unmatched disturbances, and none of the existing disturbances observers whether it is model based or not can estimate these disturbances simultaneously. In this paper, we propose a novel super twisting extended state observer (STESO) based on the concept of total disturbance estimation and rejection via ESO introduced by the author in [35]. The structure of the proposed disturbance observer combines the advantages of the super twisting algorithm [45] which guarantee robustness and fast convergence rate of the disturbance estimation with and the ESO concept which is characterized by the simplicity of its structure.

The main contributions of the paper are as follows.

(i) Developing a novel DOB based on the ESO framework which tracks the total disturbances in the system in finite time.

(ii) The chattering problem is significantly reduced by the proposed SMC-STESO controller, since the high-frequency switching gain is only required to be designed greater than the bound of the disturbance estimation rather than that of the disturbance.

(iii) Nominal performance recovery is also guaranteed by the SMC-STESO controller thanks to the STESO observer which serves like a patch to the nominal controller and does not cause any adverse effects on the system in the absence of disturbances.

(iv) Compared to the works in [46–48], our approach exploits the benefits of the extended state observer (ESO) in the diesel engine air path control problem. Indeed, by combining the sliding mode control (SMC) method with the super twisting extended state observer (STESO), the controller can achieve fast and accurate response via effective compensation for the matched and the unmatched disturbances which affect the diesel engine air path.

This paper is organized as follows. Section 2 introduces the TDE air path modeling. Section 3 describes the faulty diesel engine air path system that we are dealing with,

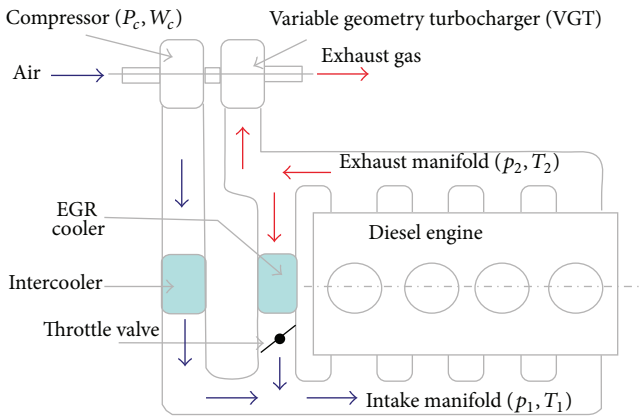

Figure 1: Turbocharged diesel engine.

together with the assumptions required. The super twisting extended state observer based sliding mode controller will be described in Section 4. Simulation results are given in Section 5. Section 6 summarizes conclusions of our work.

2. Mathematical Model of the Diesel Engine Air Path

The schematic diagram of the diesel engine is shown in Figure 1. At the top of the diagram, we can see the turbocharger and the compressor mounted on the same shaft. The turbine delivers power to the compressor by transferring the energy from the exhaust gas to the intake manifold. Together, the mixture of air from the compressor and the exhaust gas from the EGR valve with the injected fuel burn and producing the torque on the crank shaft.

The full-order TDE model is a seventh-order one which contains seven states: intake and exhaust manifold pressure (p_1 and p_2), oxygen mass fractions in the intake and exhaust manifolds (F_1 and F_2), turbocharger speed (ω_{tc}), and the two states describing the actuator dynamics for the two control signals (u_1 and u_2).

In order to obtain a simple control law, and due to the fact that the oxygen mass fraction variables are difficult to measure, the seventh-order model is reduced to a third-order one [2] presented below:

$$\begin{aligned}\dot{p}_1 &= k_1\left(W_c + W_{\text{egr}} - k_e p_1\right) + \frac{\dot{T}_1}{T_1}p_1,\\ \dot{p}_2 &= k_2\left(k_e p_1 - W_{\text{egr}} - W_t + W_f\right) + \frac{\dot{T}_2}{T_2}p_2,\\ \dot{P}_c &= \frac{1}{\tau}\left(\eta_m P_t - P_c\right),\end{aligned} \tag{1}$$

where the compressor and the turbine mass flow rate (W_c and W_t) are related to the compressor and the turbine power (P_c and P_t) as follows:

$$W_c = P_c\frac{k_c}{p_1^{\mu} - 1}, \tag{2}$$

$$P_t = k_t\left(1 - p_2^{-\mu}\right)W_t, \tag{3}$$

where

$$\begin{aligned}k_c &= \frac{\eta_c}{c_p T_a}, \qquad k_t = c_p \eta_t T_2,\\ k_1 &= \frac{R_a T_1}{V_1}, \qquad k_e = \frac{\eta_v N V_d}{R_a T_1} \quad k_2 = \frac{R_a T_2}{V_2}.\end{aligned} \tag{4}$$

Notice that the real inputs are the EGR valve and the VGT valve openings. The considered inputs, in this case for the sake of simplicity, are $u_1 = W_{\text{egr}}$ and $u_2 = W_t$, which are, respectively, the air flow through the EGR and the VGT valves.

Temperature sensors used for engine control have time constant in the order of seconds and, hence, are not fast enough to provide usable $\dot{T}_1$ and $\dot{T}_2$ signals. Moreover, steady-state values are not affected by the two terms and their dynamics can be neglected [2]. This yields to the following simplified model:

$$\begin{aligned}\dot{p}_1 &= k_1\left(W_c + W_{\text{egr}} - k_e p_1\right),\\ \dot{p}_2 &= k_2\left(k_e p_1 + W_f - W_{\text{egr}} - W_t\right),\\ \dot{P}_c &= \frac{1}{\tau}\left(\eta_m P_t - P_c\right).\end{aligned} \tag{5}$$

When replacing W_c and P_t by their expressions in (2) and (3), the simplified model can be expressed under the following control-affine form:

$$\dot{x} = f(x) + g_1(x)u_1 + g_2(x)u_2, \tag{6}$$

where $x = (p_1, p_2, P_c)^T$ and

$$f(x) = \begin{bmatrix} k_1 k_c \dfrac{P_c}{p_1^{\mu} - 1} - k_1 k_e p_1 \\ k_2\left(k_e p_1 + W_f\right) \\ \dfrac{-P_c}{\tau}\end{bmatrix}, \tag{7}$$

$$g_1(x) = \begin{bmatrix} k_1 \\ -k_2 \\ 0 \end{bmatrix}, \qquad g_2(x) = \begin{bmatrix} 0 \\ -k_2 \\ K_o\left(1 - p_2^{-\mu}\right)\end{bmatrix}, \tag{8}$$

with $K_o = (\eta_m/\tau)k_t$.

We notice that the TDE model parameters ($k_1, k_2, k_c, k_e, k_t, \tau$, and η_m) have been identified under steady-state conditions (i.e., constant engine speed and constant fueling rate) and extensive mapping. The nomenclature of the TDE parameters can be found in Table 1.

Note that in [2], the authors proved that the set Ω, defined by

$$\begin{aligned}\{\Omega = (p_1, p_2, P_c) : 1 < p_1 < P_1^{\max},\\ 1 < p_2 < p_2^{\max}, 0 < P_c < P_c^{\max}\},\end{aligned} \tag{9}$$

is an invariant set.

Table 1: Nomenclature of the diesel engine variables.

Variables	Name	Units
p_1	Intake manifold pressure	Pa
p_2	Exhaust manifold pressure	Pa
P_c	Compressor power	W
P_t	Turbine power	W
W_c	Compressor mass flow	Kg/s
W_t	Turbine mass flow	Kg/s
W_f	Fueling mass flow rate	Kg/s
η_v	Engine volumetric efficiency	—
η_c	Compressor isentropic efficiency	—
η_t	Turbine isentropic efficiency	—
η_m	Turbocharger mechanical efficiency	—
V_1	Intake manifold volume	m^3
V_2	Exhaust manifold volume	m^3
V_d	Engine volume cylinder	m^3
T_a	Ambient temperature	K
T_1	Intake manifold temperature	K
T_2	Exhaust manifold temperature	K
R_a	Specific gas constant	J/Kg/K

3. Problem Formulation

3.1. System Fault Description. In this paper, we consider the diesel engine air path model ((6), (7), and (8)) which can be written under the following control-affine form:

$$\dot{x} = f(x) + g(x)u, \tag{10}$$

where $x \in \mathbf{R}^n$, $u \in \mathbf{R}^m$ represent the state and the input vector, respectively. The vector fields f and columns g are supposed to satisfy the classical smoothness assumptions with $f(0) = 0$.

Assumption 1. System (10) is locally reachable (in the sense of [49, Definition 5, pp. 400]).

Assumption 2. A time additive actuator faults which enter the system in such a way that the faulty model can be written as

$$\dot{x} = f(x) + g(x)(u + F(x,t)), \tag{11}$$

where $F(x,t)$ is bounded by an unknown positive constant D_{m1}; that is,

$$\|F(x,t)\| < D_{m1}. \tag{12}$$

Assumption 3. The vector fields f and matrix g are dependent on the system parameters, and any uncertainties in the system parameters are reflected in them and can be expressed under the following forms:

$$\begin{aligned} \Delta f &= f(x) - f_0(x), \\ \Delta g &= g(x) - g_0(x), \\ &\text{with } \|\Delta f\| \le D_u,\ \|\Delta g\| \le D_{m2}, \end{aligned} \tag{13}$$

where f_0 and g_0 represent the nominal values of f and g and D_u, D_{m2} are the upper bounds of Δf and Δg, respectively.

Assumption 4. The external disturbances, the unmodeled dynamics, and the unknown dynamics which enters the system in different way from the control input can be expressed in an uncertain part d, so that the global faulty-disturbed model of system (10) can be written as follows:

$$\dot{x} = f(x) + g(x)(u + F(x,t)) + d. \tag{14}$$

3.2. Description of the Faulty Diesel Engine Air Path Model. In this section, we will present a description model of the faulty diesel engine air path. The faulty disturbed model considers both the actuator faults which affects directly the EGR and VGT actuators described in Assumption 2 and the uncertain part d. Following (14), the faulty disturbed diesel engine air path model is written as follows:

$$\begin{aligned} \dot{p}_1 &= k_1 W_c + k_1 u_1 - k_1 k_e p_1 + k_1 F_1, \\ \dot{p}_2 &= k_2 k_e p_1 + k_2 W_f - k_2 u_1 - k_2 u_2 - k_2 (F_1 + F_2), \\ \dot{P}_c &= \frac{-P_c}{\tau} + K_o \left(1 - p_2^{-\mu}\right)(u_2 + F_2). \end{aligned} \tag{15}$$

Clearly system (15) is under the form (14) with

$$\begin{aligned} f &= \begin{pmatrix} k_1 k_c \dfrac{P_c}{p_1^{\mu} - 1} - k_1 k_e p_1 \\ k_2 k_e p_1 \\ \dfrac{-P_c}{\tau} \end{pmatrix}, \\ g &= \begin{pmatrix} k_1 & 0 \\ -k_2 & -k_2 \\ 0 & K_o\left(1 - p_2^{-\mu}\right) \end{pmatrix}, \\ F &= \begin{pmatrix} F_1 \\ F_2 \end{pmatrix}, \qquad d = \begin{pmatrix} 0 \\ k_2 W_f \end{pmatrix}. \end{aligned} \tag{16}$$

Remark 5. (F_1, F_2) characterize the additive faults terms which affects, respectively, the EGR and the VGT actuators. Physically, it might represent a leakage which can occur on the EGR actuator and additive term which modifies the turbine flow and hence affects the VGT actuator.

Remark 6. In this work, the fueling sequence W_f is supposed to be unknown; hence, it is contained in d as an external disturbance in (15).

3.3. Control Objective and Problem Statement. For emission control, the choice of feedback variables is an important step which defines the overall controller structure. In this section, we will present our proposed air path control strategy which operates under the diesel conventional combustion mode conditions. This particular mode was characterized by the author in [48]. In this work, the author suggested that

for an optimal control performance, compressor mass flow W_c and exhaust pressure manifold p_2 are suitable choice for key output variable to be controlled. By a suitable change of coordinates, the authors in [50] proposed to replace the compressor mass flow setpoint (W_{cd}) into an intake manifold pressure setpoint (p_{1d}). This transformation simplifies the control structure by defining new vector setpoint (p_{1d}, p_{2d}). Let us now consider system (15) and define the following two sliding variables S_1, S_2

$$\begin{aligned} S_1 &= p_1 - p_{1d}, \\ S_2 &= p_2 - p_{2d}. \end{aligned} \tag{17}$$

The time derivative of S_1, S_2 along with the trajectories of the diesel faulty system (15) leads to

$$\begin{aligned} \dot{S}_1 &= k_1 W_c + k_1 u_1 - k_1 k_e p_1 + k_1 F_1 - \dot{p}_{1d}, \\ \dot{S}_2 &= k_2 k_e p_1 + k_2 W_f - k_2 u_1 - k_2 u_2 - k_2 (F_1 + F_2) - \dot{p}_{2d}. \end{aligned} \tag{18}$$

Replacing W_C by its expression in (2) yields to

$$\begin{aligned} \dot{S}_1 &= k_1 k_c \frac{P_c}{p_1^{\mu} - 1} + k_1 u_1 - k_1 k_e p_1 + k_1 F_1 - \dot{p}_{1d}, \\ \dot{S}_2 &= k_2 k_e p_1 + k_2 W_f - k_2 u_1 - k_2 u_2 - k_2 (F_1 + F_2) - \dot{p}_{2d}. \end{aligned} \tag{19}$$

The control objective of this paper can be stated as follows. Consider the faulty system (19) and the sliding manifolds $S = (S_1, S_2)^T$, and find a stabilizing closed-loop control which guarantee convergence of S toward zero in finite time.

4. Super Twisting Extended State Observer Based Sliding Mode Control Design

In this section, we will propose an observer based control design which force the sliding manifold S in (19) to converge to their reference states (p_{1d}, p_{2d}). The proposed controller combines a sliding mode feedback with a super twisting extended state observer (STESO) which estimates the total disturbances whether they are matched or unmatched. To proceed the design of STESO-SMC controller, the following lemmas are required.

Lemma 7. *For the controlled output* $[W_c, p_2]$, *the states of the zero dynamic* P_c *of the system* (15) *is stable.*

Proof. The proof of this lemma can be found in [2]. □

Lemma 8 (see [51]). *Assume that there exists a continuous positive definite function* $V(t)$ *which satisfies the following inequality:*

$$\dot{V} + \kappa_1 V(t) + \kappa_2 V^{\tau} \le 0, \quad \forall t > t_0. \tag{20}$$

Then, $V(t)$ *converges to the equilibrium point in finite time* t_s

$$t_s \le t_0 + \frac{1}{\kappa_1 (1+\tau)} \ln \frac{\kappa_1 V^{1-\tau}(t_0) + \kappa_2}{\kappa_2}, \tag{21}$$

where $\kappa_1 > 0$, $\kappa_2 > 0$ *and* $0 < \tau < 1$.

4.1. SMC Control Design. Consider now system (19) which can be rewritten under the following compact form:

$$\begin{aligned} \dot{S} = {} & f_o(x) + \left(\left(g_o(x) + \Delta g\right) u + g(x) F(x,t)\right) \\ & + \Delta f + d - \dot{S}_d, \end{aligned} \tag{22}$$

where $S = \begin{pmatrix} S_1 \\ S_2 \end{pmatrix}$, $f_0 = \begin{pmatrix} k_{1o} k_{co} (P_c / p_1^{\mu_o} - 1) - k_{1o} k_{eo} p_1 \\ k_{2o} k_{eo} p_1 \end{pmatrix}$, $g_0 = \begin{pmatrix} k_{1o} & 0 \\ -k_{2o} & -k_{2o} \end{pmatrix}$, $F = \begin{pmatrix} F_1 \\ F_2 \end{pmatrix}$, $d = \begin{pmatrix} 0 \\ k_2 W_f \end{pmatrix}$, $\dot{S}_d = \begin{pmatrix} \dot{p}_{1d} \\ \dot{p}_{2d} \end{pmatrix}$.

The control design will be achieved under the following assumptions.

Assumption 9. The states (p_1, p_2, P_c) of system (19) are available for measurements at every instant.

Assumption 10. The nominal control distribution function matrix g_0 is nonsingular.

Assumption 11. To guaranty the local reachability of system (19), the additive faults F_1, F_2 are uniquely time dependent.

System (22) contains both nominal parts f_0, g_0 which are completely known and parametric uncertainties $\Delta f, \Delta g$ and external disturbance d which are unknown for the TDE model air path. In this paper, model parametric uncertainties and disturbance are lumped together as the total disturbances, and thus, the further simplified model form for system (22) can be written as follows:

$$\dot{S} = f_0(x) + g_0(x) u + \tilde{d} - \dot{S}_d, \tag{23}$$

with $\tilde{d} = \Delta g u + g(x) F(x,t) + \Delta f + d$.

Let us now consider the following reaching law [52]:

$$\dot{S} = -\gamma S - \lambda \operatorname{sign} S, \tag{24}$$

where $S \in \mathbf{R}^2$, $u \in \mathbf{R}^2$, $\gamma = \operatorname{diag}[\gamma_1, \gamma_2]$, $\lambda = \operatorname{diag}[\lambda_1, \lambda_2]$, $\operatorname{sign} S = [\operatorname{sign}(S_1), \operatorname{sign}(S_2)]^T$.

Combining (23) and (24) yields to

$$-\gamma S - \lambda \operatorname{sign} S = f_0(x) + g_0(x) u + \tilde{d} - \dot{S}_d. \tag{25}$$

The proposed control law u is split into two parts: u_{eq} to compensate for known terms and u_n to compensate for the the lumped uncertainty $\tilde{d}$. Thus,

$$u = u_{\text{eq}} + u_n, \tag{26}$$

where

$$\begin{aligned} u_{\text{eq}} &= g_0^{-1}(x) \left(-\gamma S - \lambda \operatorname{sign} S - f_0(x) + \dot{S}_d\right), \\ u_n &= -g_0^{-1}(x) \left(\tilde{d}\right). \end{aligned} \tag{27}$$

Hence, the total control u is expressed as follows:

$$u = g_0^{-1}(x) \left(-\gamma S - \lambda \operatorname{sign} S - f_0(x) - \tilde{d} + \dot{S}_d\right). \tag{28}$$

Note that the control u_n consists of the disturbance terms $\tilde{d}$, which is completely unknown thus could not be implemented into practical systems. In order to obtain the disturbances, we will introduce the ESO to estimate it.

4.2. Super Twisting ESO Design. Following the general framework of ESO and inspired by the work in [36, 53], we design in this section an observer which estimates the total disturbances $\tilde{d}$ in (23). Adding an extended state X as the total disturbances $\tilde{d}$ to system (23) yields to the following augmented system:

$$\begin{aligned} \dot{S} &= f_0(x) + g_0(x)u + X - \dot{S}_d, \\ \dot{X} &= h(t), \end{aligned} \tag{29}$$

where $h(t)$ is the derivative of the disturbances $\tilde{d}$. For system (29), we propose the following STESO:

$$\begin{aligned} E_1 &= Z_1 - S, \\ \dot{Z}_1 &= Z_2 + f_0 + g_0 u - \dot{S}_d - \beta_1 |E_1|^{1/2} \operatorname{sign}(E_1), \\ \dot{Z}_2 &= -\beta_2 \operatorname{sign}(E_1), \end{aligned} \tag{30}$$

where $E_1 \in \mathbf{R}^2$, $Z_1 \in \mathbf{R}^2$, and $Z_2 \in \mathbf{R}^2$.

E_1 is the estimation error of the ESO, Z_1 and Z_2 are the observer internal states, and β_1 and β_2 are the observer gains. Define the observer error dynamics $E_1 = Z_1 - S$, $E_2 = Z_2 - \tilde{d}$.

Assumption 12. There exists a constants δ_1 such that

$$|h(t)| < \delta_1. \tag{31}$$

Theorem 13. *Consider the uncertain faulty augmented system* (29). *The STESO observer* (30) *ensures that the observer error* $[E_1, E_2]$ *converges to zero in a finite time if the gains* β_1, β_2 *satisfy the following conditions [54]:*

$$\begin{aligned} \beta_1 &> 0, \\ \beta_2 &> \frac{6\delta_1 + 4(\delta_1/\beta_1)^2}{2}. \end{aligned} \tag{32}$$

Proof. The observer error dynamic is given by

$$\begin{aligned} \dot{E}_1 &= Z_2 - \beta_1 |E_1|^{1/2} \operatorname{sign}(E_1) - X, \\ \dot{E}_2 &= \dot{Z}_2 - h(t), \end{aligned} \tag{33}$$

which yields to

$$\begin{aligned} \dot{E}_1 &= -\beta_1 |E_1|^{1/2} \operatorname{sign}(E_1) + E_2, \\ \dot{E}_2 &= -\beta_2 \operatorname{sign}(E_1) + \rho_1, \end{aligned} \tag{34}$$

with $\rho_1 = -h(t)$.

It is easy to see that system (34) is under the generalized super twisting algorithm differential inclusion and it is finite time stable (see [54]). This completes the proof. □

Remark 14. The class of disturbances considered in this paper is much larger than the ones considered [44] where it is assumed that the disturbances are bounded and their derivatives vanish as $t \to \infty$. It may be noted that it is not required to know the bound δ_1.

Remark 15. We notice that the expression of Z_2 in (30) shows that Z_2 can estimate (or track) the total action of the uncertain models and the external disturbances $\tilde{d}$ in finite time. As Z_2 is the estimation for the total action of the unknown disturbances, in the feedback, Z_2 is used to compensate the disturbances.

With the disturbances $\tilde{d}$ estimated by the STESO, the control law (28) is modified as follows:

$$u = g_0^{-1}(x)\left(-\gamma S - \lambda \operatorname{sign} S - f_0(x) - Z_2 + \dot{S}_d\right). \tag{35}$$

4.3. Stability Analysis of Closed-Loop Dynamics. Replacing the control law (35) in (23) yields to the following closed-loop system:

$$\dot{S} = -\gamma S - \lambda \operatorname{sign} S + \left(\tilde{d} - Z_2\right), \tag{36}$$

which can be written as follows:

$$\dot{S} = -\gamma S - \lambda \operatorname{sign} S - E_2. \tag{37}$$

Theorem 16. *For the plant* (23) *with the control law* (35) *and the STESO observer* (30), *the trajectory of the closed-loop system* (37) *can be driven to the origin in finite time.*

Proof. Consider the following Lyapunov function:

$$V = \frac{1}{2} S(t)^T S(t). \tag{38}$$

□

Taking the derivative of (38) yields to

$$\begin{aligned} \dot{V} &= S(t)^T (-\gamma S - \lambda \operatorname{sign} S - E_2) \\ &= -\sum_{i=1}^{2} \left(\gamma_i S_i^2 + \lambda_i |S_i|\right) - S^T E_2 \\ &\le -\sum_{i=1}^{2} \gamma_i S_i^2 - \sum_{i=1}^{2} (\lambda_i - |E_{2i}|) |S_i|. \end{aligned} \tag{39}$$

Choosing $\lambda_i > |E_{2i}|$ ensures by Lemma 8 the finite time stability of the sliding manifolds S.

Remark 17. Since the disturbance has been precisely estimated by the STESO, the magnitude of the estimation error E_{2i} which converges to 0 can be kept much smaller than the magnitude of the disturbance $\tilde{d}$; this will alleviate the chattering phenomenon.

Remark 18 (Performance Nominal Recovery). In the absence of disturbance, it is derived from the observer error dynamics (34); that is, $E_{2i} \to 0$. In this case, the closed-loop dynamics (37) reduces to those of the traditional sliding mode control (TSMC). This implies that the nominal control performance of the proposed method is retained.

Table 2: Control requirements for the STESO-SMC controller.

Variable	Setpoint 1	Setpoint 2
W_{cd} (Kg/s)	0.03	0.04
P_{2d} (Bar)	1.45	1.75

5. Simulation and Evaluation

In this section, we report numerical results obtained from the simulation of controller (35) on the reduced third-order model developed in ((1)–(8)). The engine used is a common rail direct-injection in-line-4-cylinder provided by a French manufacturer. Numerical values of (η_t, η_c, η_v, and η_m) cartographies in the TDE model were provided by the manufacturer. The model parameters nominal values k_{o1}, k_{o2}, k_{oc}, k_{oe}, k_{ot}, τ_o, η_{om}, and μ_o are usually identified around some given operating points. In these simulations, the parameters of the model ((1)–(8)) were taken from [6]; that is, $k_{o1} = 143.91$, $k_{o2} = 1715.5$, $k_{oc} = 0.0025$, $k_{oe} = 0.028$, $k_{ot} = 391.365$, $\tau_o = 0.15$, $\eta_{om} = 0.95$, and $\mu_o = 0.285$. A well-known continuous approximation of the function sign(S) is given by

$$\text{Sign}(S) = \frac{s}{|s| + \xi}. \tag{40}$$

This approximation is used to ensure that the sliding motion will be in the vicinity of the line ($S = 0$). In this simulation, the approximation of the sign function has been implemented with $\xi = 0.01$. The simulations were conducted under the control requirements defined in Table 2.

In this section, we mention that numerical simulations were performed in real-time software in the loop (SIL) using the dSpace modular simulator. This real-time platform is based on the DS-1006 board interfaced with MATLAB/Simulink software. The controller (35) and the TDE third-order model run on this platform with a sampling step time equal to 10^{-4} s. For the purpose of simulations, parametric uncertainties Δf and actuator faults F were chosen under periodic forms (like sinus). The goal was to only prove the effectiveness of the STESO observer and the controller (35). From a practical point of view, it is very difficult to model either a leakage affecting the EGR and the VGT actuators or parametric uncertainties affecting the TDE air path model. We cannot also say that the EGR and the VGT actuator faults are periodic; however, and as stated in Remark 14, the only assumption we made on the total disturbances $\tilde{d}$ is on its time derivatives which must be bounded. Thus, complex leakage or parametric uncertainties forms which can be more realistic can be considered in practical situations.

Case 1 (traditional SMC control versus STESO-SMC control in case of matched disturbances). In this simulation, we wanted to compare the performance of the STESO-SMC and the traditional SMC controllers in the case where only matched disturbances are considered. The two controllers were simulated under nominal parametric values (i.e., $\Delta f = 0$ and $\Delta g = 0$) and fueling sequence $W_f = 0$.

Table 3: Control gains of the TSMC and the STESO-SMC controllers in Case 1.

Controllers	Controllers parameters	
TSMC	$\lambda = 100$	$\gamma = 250$
STESO-SMC	$\lambda = 3$	$\gamma = 250$

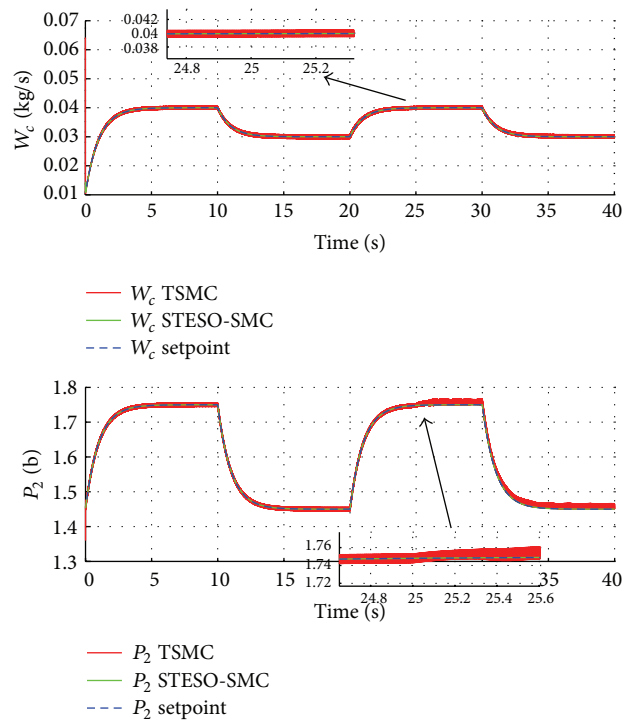

Figure 2: Controlled variables W_c, p_2 in Case 1.

The considered matched disturbances were a time varying additive leakage which takes the following form:

$$F(t) = \begin{cases} 0 \times (1,1)^T & \text{if } t < 25 \text{ s} \\ -0.04 + 0.01 \sin(0.2\pi t) \times (1,1)^T & \text{if } t \geq 25 \text{ s.} \end{cases} \tag{41}$$

For the TSMC and the STESO-SMC controllers, the gains λ, γ (see Table 3) were tuned in order to get an equivalent tracking performance for the controlled variables W_c and p_2.

Response curves of the two controlled variables W_c, p_2 are shown in Figure 2. A brief observation from Figure 2 shows that for $t < 25$ s, the STESO-SMC controller exhibits the same level of tracking performance comparing to the TSMC one. When the faults occur, it can be observed from Figure 2 that the proposed STESO-SMC obtains fine disturbance rejection property with minimal chattering effects, while the TSMC keeps well the tracking performance of W_c, p_2 but pay high price in terms of chattering due to the higher value of the switching gain λ needed for the TSMC in order to counteract the occurrence of the faults at $t = 25$ s.

This can be observed in Figure 3 where we can see that the control effort (U_{egr}, U_{vgt}) produced by the STESO-SMC

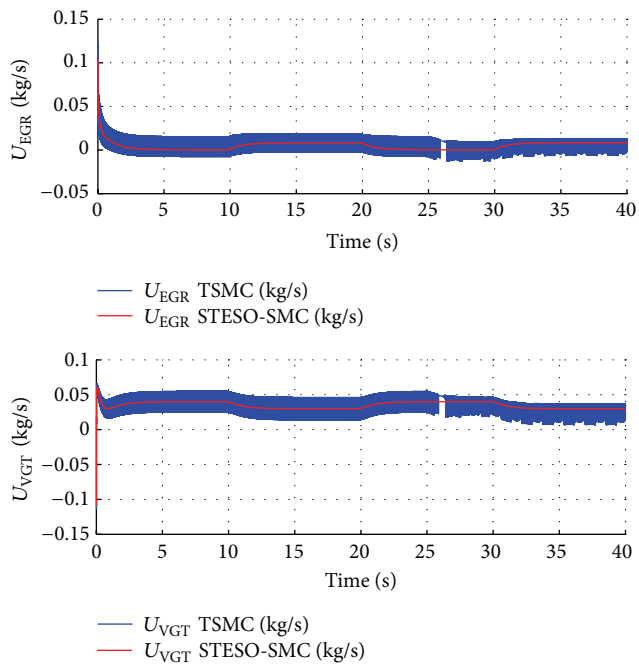

Figure 3: Control effort of the EGR and the VGT actuators for the TSMC and the STESO-SMC controllers.

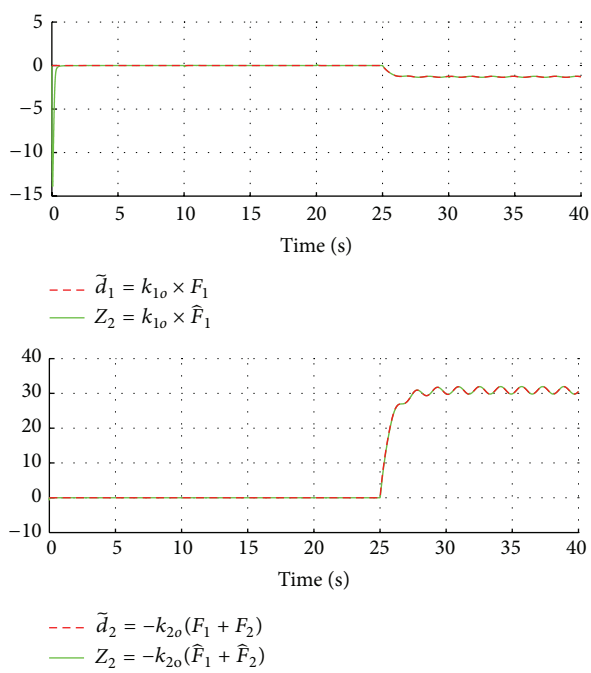

Figure 4: Estimation of matched disturbances via STESO in Case 1.

controller is characterized by the low level of the chattering comparing to the TSMC one.

When only matched disturbances are considered, the total disturbance $\tilde{d}$ in system (23) is expressed as follows:

$$\tilde{d} = \begin{pmatrix} k_{1o}F_1 \\ -k_{2o}F_1 - k_{2o}F_2 \end{pmatrix}. \tag{42}$$

Selecting appropriate values of $\beta_{11} = \beta_{21} = \beta_{12} = \beta_{22} = 1000$ for the STESO observer, one can observe from Figure 4 that it can estimate the total disturbance accurately even if there exist some small shocks due to the drastic changes which occur on the vector derivatives $\dot{S}_d$. It is important to mention that the tracking performance and the disturbance rejection of the STESO-SMC depend on the estimation of $\tilde{d}$ provided by the STESO.

Case 2 (performance of the STESO-SMC Control in presence of unmatched disturbances and matched disturbances). In this simulation, we wanted to show the performance of the STESO-SMC controller when both matched and unmatched disturbances are considered. To the matched disturbances considered in Case 1, we assume also the following unmatched disturbances.

(i) Parametric variation Δf takes the following form:

$$\Delta f = \begin{pmatrix} 0.2 \sin(0.2\pi p_1 t) \\ 0.5 \sin(0.3\pi p_2 t) \end{pmatrix}. \tag{43}$$

(ii) Fueling sequence takes the following form:

$$W_f = \begin{cases} 0\,\text{kg/h} & \text{if } t < 5\,\text{s} \\ 7\,\text{kg/h} & \text{if } t \geq 5\,\text{s}. \end{cases} \tag{44}$$

Hence, the total disturbance $\tilde{d}$ in system (23) at different time, is expressed as follows.

For $t < 5$ s,

$$\tilde{d} = \begin{pmatrix} \Delta f_1 \\ \Delta f_2 \end{pmatrix}. \tag{45}$$

For $5 < t < 25$ s,

$$\tilde{d} = \begin{pmatrix} \Delta f_1 \\ k_{2o}W_f + \Delta f_2 \end{pmatrix}. \tag{46}$$

For $t \geq 25$ s,

$$\tilde{d} = \begin{pmatrix} \Delta f_1 + k_{1o}F_1 \\ \Delta f_2 + k_{2o}W_f - k_{2o}F_1 - k_{2o}F_2 \end{pmatrix}. \tag{47}$$

To test the nominal performance recovery, the total disturbances $\tilde{d}$ whether it is matched or unmatched is nullified at $t = 35$ s.

Figure 5 shows the response curves of the two controlled variables W_c, p_2 when both matched and matched uncertainties are considered. In this simulation, we mention that the control parameters λ, γ were kept the same as in Case 1 ($\lambda = 3, \gamma = 250$). A brief observation from Figure 5 shows that the STESO-SMC controller successfully rejects from the beginning of the simulation the matched and the unmatched disturbances thanks to the action of STESO. A comparison between the performance of the STESO-SMC in Cases 1 and 2 (see Figures 2 and 5) shows that the STESO-SMC controller exhibits the same level of tracking performance despite the fact that in Case 2 unmatched disturbances were added to the plant. This remark can be explained by the fact that the

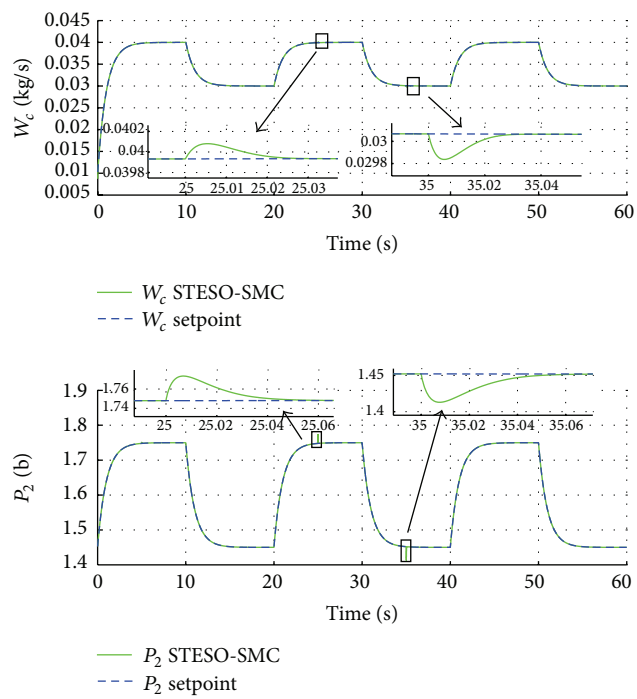

FIGURE 5: Controlled variables W_c, p_2 in Case 2.

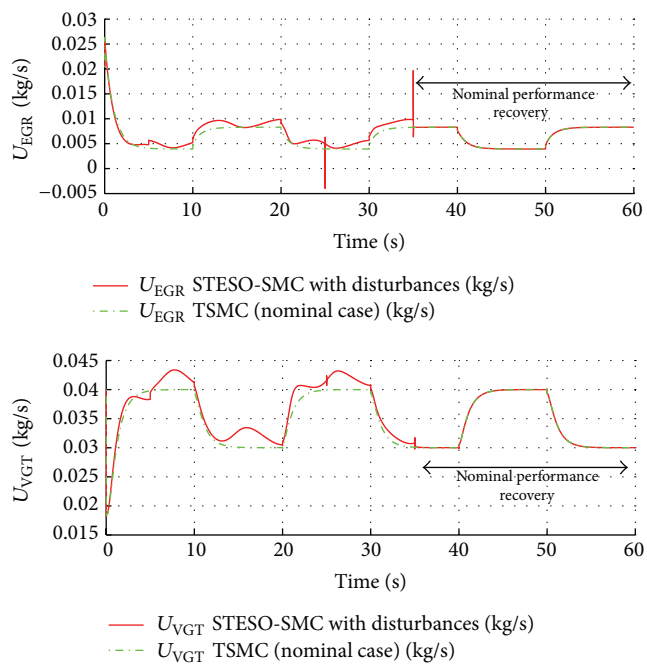

FIGURE 6: Control effort of the EGR and the VGT actuators for the TSMC (nominal case) and the STESO-SMC controllers in Case 2.

control parameters (λ, γ) were maintained the same as it was in Case 1 and since the STESO converges ($E_{2i} \rightarrow 0$), whether matched and unmatched disturbances are considered, the closed-loop dynamics in Cases 1 and 2 is the same.

Figure 6 shows the control effort (U_{egr}, U_{vgt}) produced by the STESO-SMC controller in Case 2. It can be observed from Figure 6 that the STESO-SMC manages to compensate the matched and the unmatched disturbances from the beginning of the simulation. When we nullified all the disturbances which affect the plant at $t = 35$ s, we could see that the two controls produced by the STESO-SMC and TSMC in nominal case are the same. This means that the STESO-SMC recovers the nominal performances which validates Remark 18.

Figure 7 shows the performance of the STESO in terms of estimating the total disturbances in Case 2. We keep the same values $\beta_{11} = \beta_{21} = \beta_{12} = \beta_{22} = 1000$ for the STESO in this case. One can observe from Figure 7 that there is a good tracking of the disturbances from the beginning of the simulation. We conclude by noticing that the performance of the STESO-SMC controllers depend on the control parameters (λ, γ) and the STESO gains $\beta_{11}, \beta_{21}, \beta_{12}$, and β_{22}. Each of them can be tuned separately without a compromise between the chattering problem and the convergence of the sliding surface. Indeed, to alleviate the chattering, the control parameters required to be only greater than the disturbances error and to ensure fast convergence of the sliding surface the STESO gains can be chosen so that we get a fast convergence of the disturbance error which lead to fast convergence of the sliding surface.

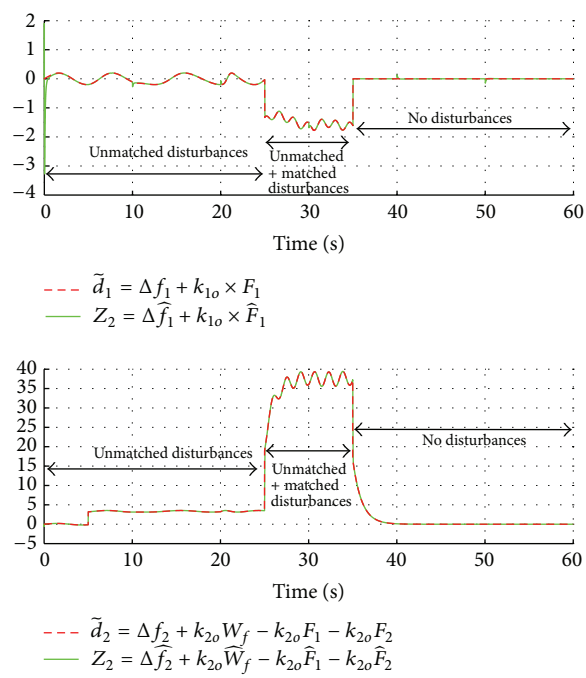

FIGURE 7: Estimation of matched and unmatched disturbances via STESO in Case 2.

6. Conclusions

In this paper, a novel DOB based SMC, namely, STESO-SMC, controller has been proposed to attenuate the matched and the unmatched disturbances for the purpose of controlling the diesel engine air path. The main contribution here is

the design of a new STESO observer in such a way that the sliding motion along the sliding surface can drive the states to their desired trajectories in finite time. As compared with the traditional SMC, the proposed controller has exhibited two superiorities in the simulation including nominal performance recovery and chattering effect reduction.

Conflict of Interests

The authors declare that there is no conflict of interests regarding the publication of this paper.

Acknowledgments

The authors gratefully thank Region Haute-Normandie OSEO and FEDER for financially supporting this work and its forthcoming application to an ICE control within the framework of the VIRTUOSE Project.

References

[1] L. Eriksson, J. Wahlström, and L. Nielsen, "EGR-VGT control and tuning for pumping work minimization and emission control," *IEEE Transactions on Control Systems Technology*, vol. 18, no. 4, pp. 993–1003, 2010.

[2] M. Jankovic, M. Jankovic, and I. Kolmanovsky, "Constructive Lyapunov control design for turbocharged diesel engines," *IEEE Transactions on Control Systems Technology*, vol. 8, no. 2, pp. 288–299, 2000.

[3] M. Jung and K. Glover, "Calibratable linear parameter-varying control of a turbocharged diesel engine," *IEEE Transactions on Control Systems Technology*, vol. 14, no. 1, pp. 45–62, 2006.

[4] L. Lihua, W. Xiukun, and L. Xiaohe, "LPV control for the air path system of diesel engines," in *Proceedings of the IEEE International Conference on Control and Automation (ICCA '07)*, pp. 873–878, June 2007.

[5] X. Wei and L. del Re, "Gain scheduled H_∞ control for air path systems of diesel engines using LPV techniques," *IEEE Transactions on Control Systems Technology*, vol. 15, no. 3, pp. 406–415, 2007.

[6] M. Larsen, M. Jankovic, and P. V. Kokotovic, "Indirect passivation design for diesel engine model," in *Proceedings of the 2000 IEEE International Conference on Control Applications*, pp. 309–314, 2000.

[7] H. J. Ferreau, P. Ortner, P. Langthaler, L. D. Re, and M. Diehl, "Predictive control of a real-world Diesel engine using an extended online active set strategy," *Annual Reviews in Control*, vol. 31, no. 2, pp. 293–301, 2007.

[8] A. Plianos, A. Achira, R. Stobart, N. Langlois, and H. Chafouk, "Dynamic feedback linearization based control synthesis of the turbocharged Diesel engine," in *Proceedings of the IEEE American Control Conference (ACC '07)*, pp. 4407–4412, July 2007.

[9] M. Dabo, N. Langlois, and H. Chafouk, "Dynamic feedback linearization applied to asymptotic tracking: generalization about the turbocharged diesel engine outputs choice," in *Proceedings of the IEEE American Control Conference (ACC '09)*, pp. 3458–3463, June 2009.

[10] L. Guzzella and A. Amstutz, "Control of diesel engines," *IEEE Control Systems Magazine*, vol. 18, no. 5, pp. 53–71, 1998.

[11] M. Kao and J. J. Moskwa, "Turbocharged diesel engine modeling for nonlinear engine control and state estimation," *Journal of Dynamic Systems, Measurement and Control*, vol. 117, no. 1, pp. 20–30, 1995.

[12] I. V. Kolmanovsky, P. E. Moraal, M. J. van Nieuwstadt, and A. Stefanopoulou, "Issues in modelling and control of intake flow in variable geometry turbocharged engines," in *Proceedings of the 18th IFIP conference on system modelling and optimization*, pp. 436–445, 1997.

[13] P. E. Moraal, M. J. van Nieuwstadt, and I. V. Kolmanovsky, "Modelling and control of a variable geometry turbocharged diesel engine," in *Proceedings of the COSY Workshop, European Control Conference*, 1997.

[14] V. I. Utkin, "Variable structure systems with sliding mode: a survey," *IEEE Transactions on Automatic Control*, vol. 22, no. 5, pp. 212–222, 1977.

[15] J. Y. Hung, W. Gao, and J. C. Hung, "Variable structure control. A survey," *IEEE Transactions on Industrial Electronics*, vol. 40, no. 1, pp. 2–22, 1993.

[16] X. Yu and O. Kaynak, "Sliding-mode control with soft computing: a survey," *IEEE Transactions on Industrial Electronics*, vol. 56, no. 9, pp. 3275–3285, 2009.

[17] A. Pisano and E. Usai, "Sliding mode control: a survey with applications in math," *Mathematics and Computers in Simulation*, vol. 81, no. 5, pp. 954–979, 2011.

[18] S. Islam and X. P. Liu, "Robust sliding mode control for robot manipulators," *IEEE Transactions on Industrial Electronics*, vol. 58, no. 6, pp. 2444–2453, 2011.

[19] N. Chen, F. Song, G. Li, X. Sun, and C. Ai, "An adaptive sliding mode backstepping control for the mobile manipulator with nonholonomic constraints," *Communications in Nonlinear Science and Numerical Simulation*, vol. 18, no. 10, pp. 2885–2899, 2013.

[20] M. L. Corradini, V. Fossi, A. Giantomassi, G. Ippoliti, S. Longhi, and G. Orlando, "Discrete time sliding mode control of robotic manipulators: development and experimental validation," *Control Engineering Practice*, vol. 20, pp. 816–822, 2012.

[21] Z. Zhang, H. Xu, L. Xu, and L. E. Heilman, "Sensorless direct field-oriented control of three-phase induction motors based on "sliding mode" for washing-machine drive applications," *IEEE Transactions on Industry Applications*, vol. 42, no. 3, pp. 694–701, 2006.

[22] O. Barambones and P. Alkorta, "A robust vector control for induction motor drives with an adaptive sliding-mode control law," *Journal of the Franklin Institute*, vol. 348, no. 2, pp. 300–314, 2011.

[23] R. Wai and L. Shih, "Design of voltage tracking control for DC-DC boost converter via total sliding-mode technique," *IEEE Transactions on Industrial Electronics*, vol. 58, no. 6, pp. 2502–2511, 2011.

[24] Y. Shtessel, S. Baev, and H. Biglari, "Unity power factor control in three-phase AC/DC boost converter using sliding modes," *IEEE Transactions on Industrial Electronics*, vol. 55, no. 11, pp. 3874–3882, 2008.

[25] B. Xiao, Q. Hu, and Y. Zhang, "Adaptive sliding mode fault tolerant attitude tracking control for flexible spacecraft under actuator saturation," *IEEE Transactions on Control Systems Technology*, vol. 20, pp. 1605–1612, 2012.

[26] Q. Hu, "Adaptive output feedback sliding-mode manoeuvring and vibration control of flexible spacecraft with input saturation," *IET Control Theory & Applications*, vol. 2, no. 6, pp. 467–478, 2008.

[27] H. H. Choi, "LMI-based sliding surface design for integral sliding mode control of mismatched uncertain systems," *IEEE Transactions on Automatic Control*, vol. 52, no. 4, pp. 736–742, 2007.

[28] C. Johnson, "Accommodation of external disturbances in linear regulator and servomechanism problems," *IEEE Transactions on Automatic Control*, vol. 16, no. 6, pp. 635–644, 1971.

[29] W. Chen, "Disturbance observer based control for nonlinear systems," *IEEE/ASME Transactions on Mechatronics*, vol. 9, no. 4, pp. 706–710, 2004.

[30] L. Guo and W. Chen, "Disturbance attenuation and rejection for systems with nonlinearity via DOBC approach," *International Journal of Robust and Nonlinear Control*, vol. 15, no. 3, pp. 109–125, 2005.

[31] S. J. Kwon and W. K. Chung, "A discrete-time design and analysis of perturbation observer for motion control applications," *IEEE Transactions on Control Systems Technology*, vol. 11, no. 3, pp. 399–407, 2003.

[32] J. She, X. Xin, and Y. Pan, "Equivalent-input-disturbance approachanalysis and application to disturbance rejection in dual-stage feed drive control system," *IEEE Transactions on Mechatronics*, vol. 16, no. 2, pp. 330–340, 1998.

[33] T. Floquet, C. Edwards, and S. K. Spurgeon, "On sliding mode observers for systems with unknown inputs," in *Proceedings of the International Workshop Variable Structure System*, pp. 5–7, 2006.

[34] J. Han, "Extended state observer for a class of uncertain plants," *Control and Decision*, vol. 10, no. 1, pp. 85–88, 1995.

[35] J. Han, "From PID to active disturbance rejection control," *IEEE Transactions on Industrial Electronics*, vol. 56, no. 3, pp. 900–906, 2009.

[36] D. Sun, "Comments on active disturbance rejection control," *IEEE Transactions on Industrial Electronics*, vol. 54, no. 6, pp. 3428–3429, 2007.

[37] Y. Xia, P. Shi, G. P. Liu, D. Rees, and J. Han, "Active disturbance rejection control for uncertain multivariable systems with time-delay," *IET Control Theory and Applications*, vol. 1, no. 1, pp. 75–81, 2007.

[38] S. Li, J. Yang, W. H. Chen, and X. Chen, "Generalized extended state observer based control for systems with mismatched uncertainties," *IEEE Transaction on Industrial Electronics*, vol. 56, no. 12, pp. 4792–4802, 2012.

[39] X. Wei and L. Guo, "Composite disturbance-observer-based control and terminal sliding mode control for non-linear systems with disturbances," *International Journal of Control*, vol. 82, no. 6, pp. 1082–1098, 2009.

[40] M. Chen and W.-H. Chen, "Sliding mode control for a class of uncertain nonlinear system based on disturbance observer," *International Journal of Adaptive Control and Signal Processing*, vol. 24, no. 1, pp. 51–64, 2010.

[41] S. Li, K. Zong, and H. Liu, "A composite speed controller based on a second-order model of permanent magnet synchronous motor system," *IEEE Transactions on Instrumentation, Measure and Control*, vol. 33, no. 5, pp. 522–541, 2011.

[42] Y. Lu, "Sliding-mode disturbance observer with switching-gain adaptation and its application to optical disk drives," *IEEE Transactions on Industrial Electronics*, vol. 56, no. 9, pp. 3743–3750, 2009.

[43] Y. Lu and C. Chiu, "A stability-guaranteed integral sliding disturbance observer for systems suffering from disturbances with bounded first time derivatives," *International Journal of Control, Automation and Systems*, vol. 9, no. 2, pp. 402–409, 2011.

[44] J. Yang, S. Li, and X. Yu, "Sliding-mode control for systems with mismatched uncertainties via a disturbance observer," *IEEE Transaction on Industrial Electronics*, vol. 60, pp. 160–169, 2013.

[45] L. Fridman and A. Levant, "Higher order sliding modes," in *Sliding Mode Control in Engineering*, chapter 3, pp. 53–101, Marcel Dekker, 2002.

[46] V. I. Utkin, H. Chang, I. Kolmanovsky, and J. A. Cook, "Sliding mode control for variable geometry turbocharged diesel engines," in *Proceedings of the IEEE American Control Conference (ACC '00)*, pp. 584–588, June 2000.

[47] D. Upadhyay, V. I. Utkin, and G. Rizzoni, "Multivariable control design for intake flow regulation of a diesel engine using sliding mode," in *Proceedings of the 15th Triennal IFAC World Congress*, pp. 1389–1394, 2002.

[48] J. Wang, "Hybrid robust air-path control for diesel engines operating conventional and low temperature combustion modes," *IEEE Transactions on Control Systems Technology*, vol. 16, no. 6, pp. 1138–1151, 2008.

[49] M. Vidyasagar, *Nonlinear Systems Analysis*, Prentice-Hall, Englewood Cliffs, NJ, USA, 2nd edition, 1993.

[50] S. A. Ali, B. N'doye, and N. Langlois, "Sliding mode control for turbocharged diesel engine," in *Proceedings of the Internationnal Conference on Control and Automation (MED)*, pp. 996–1001, 2012.

[51] M. Zhihong and X. H. Yu, "Terminal sliding mode control of MIMO linear systems," *IEEE Transactions on Circuits and Systems I*, vol. 44, no. 11, pp. 1065–1070, 1997.

[52] W. Gao and J. C. Hung, "Variable structure control of nonlinear systems. A new approach," *IEEE Transactions on Industrial Electronics*, vol. 40, no. 1, pp. 45–55, 1993.

[53] Y. Xia, Z. Zhu, M. Fu, and S. Wang, "Attitude tracking of rigid spacecraft with bounded disturbances," *IEEE Transactions on Industrial Electronics*, vol. 58, no. 2, pp. 647–659, 2011.

[54] J. A. Moreno and M. Osorio, "A Lyapunov approach to second-order sliding mode controllers and observers," in *Proceedings of the 47th IEEE Conference on Decision and Control (CDC '08)*, pp. 2856–2861, December 2008.